PREDICTION OF INELASTIC SEISMIC RESPONSES OF ARCH-TYPE LONG-SPAN STRUCTURES USING A SERIES OF MULTIMODAL PUSHOVER ANALYSES

M. Ohsaki and J. Y. Zhang

Department of Architecture, Hiroshima University, Japan
Graduate School of Architecture and Design, Nagoya City University, Japan

Editor's Note: This space reserved for the Editor to give such information as date of receipt of manuscript, date of receipt of revisions (if any), and date of acceptance of paper.

ABSTRACT

A new approach is presented for evaluating seismic responses of arch-type long-span structures. The responses are estimated by a series of pushover analyses utilizing multiple load patterns as linear combinations of dominant modes. The representative displacement and acceleration are defined in a general manner without using the base shear or roof displacement. The eigenmodes of initial elastic structure are used for assembling the equivalent static loads to take the snapshot of the deformed structure at the maximum deformation. The damping due to plastic energy dissipation is modeled by equivalent linearization for inelastic systems. Accuracy of the proposed method, especially for force and stress responses, is demonstrated in the numerical example of an arch-type long-span truss.

Keywords: Pushover analysis, multiple modes, seismic response, equivalent static load, long-span structure

1. INTRODUCTION

In the seismic design process of long-span structures, including arches and latticed shells, the maximum values of responses such as displacements and stresses under seismic motions are evaluated using time-history analysis. However, a time-history analysis can confirm the responses to the specific motion; accordingly, it does not reveal general and average properties of the seismic responses of the structure, although it demands a substantial computational cost. In contrast, for building structures, a static analysis called pushover analysis is used to evaluate the inelastic responses under monotonically increasing seismic loads. Therefore, it is convenient to use pushover analysis for long-span structures in a similar manner as building structures.

It is important that several dominant modes should be considered in evaluation of seismic responses of long-span structures [1,2]. In contrast, the lowest mode dominates in building structures. However, several methods have recently been developed for incorporating higher modes for seismic design of building structures. Hence, we can extend such methods to be applicable to long-span structures.

If the responses are in elastic range, the maximum responses can be obtained using the Square-Root-of-Sum-of-Squares (SRSS) rule, or preferably the Complete Quadratic Combination (CQC) rule [3], when the frequencies of the dominant modes are closely spaced. For inelastic systems, however, a nonlinear static pushover analysis with fixed pattern is usually adopted. Three problems then arise in this procedure: (1) how to deal with the change of mode shape after redistribution of inertia force due to plastification, (2) how to determine the rule for modal combination, and (3) when to terminate the process of pushover analysis.

For the first problem, several methods of adaptive pushover analysis have been proposed to modify the load pattern after plastification [4-6]. There are two approaches to overcome the second problem: (a) combine modes to define the static load pattern before pushover analysis, (b) combine the response against each dominant mode after pushover analysis. Various methodologies have been presented for incorporating multiple modes, or the change of load distribution due to plastification of building frames.

Chopra and Goel [7] proposed a method of multimodal pushover analysis (MPA), where the responses of several modes are computed by the pushover analysis that are combined using the SRSS rule; however, in this method, the response of a less dominant mode remains in an elastic range and may be underestimated in prediction of elastoplastic responses. MPA has also been extended to three-dimensional structures utilizing three-dimensional version of CQC method [8], and to estimation of member forces by local correction utilizing the stress-strain relation [9]. However, it is very difficult to estimate the maximum response induced by seismic motions by a pushover analysis of an only one load pattern.

Some parametric studies have been done to find the optimal combination coefficients for response prediction [10,11]. Kunnath [10] presented a method to take a snapshot of the deformation at which a response quantity has the maximum value using three modes. In FEMA-356 [12], it is recommended to use more than two patterns among the three patterns of uniform, triangular, and modal combination by SRSS or CQC rule. Eurocode 8 [13] also recommends the use of multiple load patterns.

Regarding the third problem above, the capacity spectrum method (CSM) is usually used for incorporating the energy dissipation after plastification [14,15]. Similar approach called Calculation of Response and Limit Strength is used in Japan based on Notification 1457 of the Ministry of Land, Infrastructure and Transport (MLIT).

For long-span structures, Nakazawa *et al.* [16] presented modal pushover analysis and adaptive modal pushover analysis. Kato *et al.* [17] applied MPA to latticed domes. However, it is difficult to define the representative displacement and acceleration (force) for long-span structures, because their vertical components against horizontal seismic motions should be appropriately incorporated; hence, the base shear and roof displacement in horizontal direction cannot be used. Uchida *et al.* [18] and Zhang *et al.* [19] presented a general definition of the representative displacement and acceleration that are applicable to long-span structures, which have multiple dominant modes.

In this paper, we present a general approach to evaluation of mean-maximum responses of long-span structures utilizing several load patterns. The representative displacement and acceleration are defined in a general manner without using roof displacement or base shear. It is shown that the maximum responses, including forces and stresses, of a long-span arch-type truss are successfully evaluated by carrying out static pushover analyses several times.

2. DEFINITION OF DOMINANT MODES

Consider a structure subjected to base acceleration $\ddot{u}_{\mathrm{g}}(t)$, which is a function of time t. The mass matrix, damping matrix, and stiffness matrix are denoted by $\mathbf{M}$, $\mathbf{C}$, and $\mathbf{K}$, respectively. The vectors of relative displacement, velocity, and acceleration from the base are denoted by $\mathbf{u}(t)$, $\dot{\mathbf{u}}(t)$, and $\ddot{\mathbf{u}}(t)$, respectively. Let $\mathbf{I}$ denote the vector, in which the components corresponding to the input direction are 1, and the remaining components are 0. Then, the equation of motion is written as

$$\mathbf{M}\ddot{\mathbf{u}}(t)+\mathbf{C}\dot{\mathbf{u}}(t)+\mathbf{K}\mathbf{u}(t)=-\mathbf{M}\mathbf{I}\ddot{u}_{\mathrm{g}}(t) \tag{1}$$

Let Φ_n denote the n th mode of undamped free vibration, which is orthonormalized by

$$\Phi_i^\top \mathbf{M}\Phi_j=\delta_{ij} \tag{2}$$

where δ_{ij} is the Kronecker delta. The participation factor Γ_n and the effective modal mass M_n of the n th mode are defined as

$$\Gamma_n=\Phi_n^\top \mathbf{M}\mathbf{I},\ \ M_n=(\Gamma_n)^2 \tag{3}$$

The time history of relative displacement and acceleration vectors $\mathbf{u}(t)$ and $\ddot{\mathbf{u}}(t)$, respectively, are approximated using the modal responses $\Gamma_n D_n(t)$ and $\Gamma_n A_n(t)$ with the coefficients $D_n(t)$ and $A_n(t)$ as

$$\mathbf{u}(t)=\sum_{n=1}^{N}\Gamma_n D_n(t)\Phi_n,\ \ \ddot{\mathbf{u}}(t)=\sum_{n=1}^{N}\Gamma_n A_n(t)\Phi_n \tag{4a,b}$$

where we assume, for simplicity, that N lowest modes are used.

In the current practical design process, the magnitude and dynamic characteristics of the seismic motions are specified by the design acceleration spectrum. Let ω_n denote the n th natural circular frequency. The design acceleration response spectrum is given as a function of natural circular frequency as $S^{\mathrm{a}}(\omega_n)$. Then, the pseudo-displacement response spectrum $S^{\mathrm{d}}(\omega_n)$ is defined as

$$S^{\mathrm{d}}(\omega_n) = \frac{1}{\omega_n^2} S^{\mathrm{a}}(\omega_n) \tag{5}$$

The effective mass ratio ρ_n and the maximum strain energy E_n of the n th mode are defined as

$$\rho_n = \frac{M_n}{\mathbf{I}^\top \mathbf{M} \mathbf{I}}, \; E_n = \frac{1}{2} M_n (\omega_n S^{\mathrm{d}}(\omega_n))^2 \tag{6}$$

The mode with large values of E_n and ρ_n are selected as dominant modes.

Let $\mathbf{f}_{n0}$ denote the static load vector corresponding to the n th mode. The static seismic load $\mathbf{f}_0$ is defined as a linear combination of $\mathbf{f}_{n0}$ with coefficients α_n as

$$\mathbf{f}_0 = \sum_{n=1}^{N} \alpha_n \mathbf{f}_{n0}, \; \mathbf{f}_{n0} = \Gamma_n S^{\mathrm{a}}(\omega_n) \mathbf{M} \Phi_n \tag{7}$$

If damping is not very large, any deformed shape of an elastic structure can be expressed as a linear combination of dominant modes, which can be found by applying the seismic load $\mathbf{f}_0$ defined in Eq.(7) statically. Therefore, the process of finding the maximum value of each response displacement component is reduced to that of determining the coefficients α_n appropriately to take the snapshot of the deformed shape at the maximum displacement.

3. ESTIMATION OF INELASTIC RESPONSE USING EQUIVALENT LINEARIZATION

3.1 Multimodal Pushover Analysis

In most of the static estimation methods of inelastic dynamic responses, including MPA, the modal responses are computed independently using a nonlinear pushover analysis with incremental load coefficient, and they are combined using the SRSS rule. The roof displacement and base shear are used as the representative displacement and force (acceleration) for a regular building frame to draw the force-displacement curve. However, for long-span structures, vertical displacements and forces sometimes dominate over the horizontal ones; hence, more appropriate representative displacement and force should be defined.

Let $\mathbf{u}^i$ and $\mathbf{a}^i$ denote the vectors of nodal displacements and accelerations at the i th step of pushover analysis, where $\mathbf{a}^i$ is obtained by dividing the nodal force by the corresponding nodal mass. The vector $\mathbf{u}^i$ is normalized to a mode $\mathbf{u}_0^i$ as

$$\mathbf{u}_0^i = \frac{1}{\sqrt{\mathbf{u}^{i\top} \mathbf{M} \mathbf{u}^i}} \mathbf{u}^i \tag{8}$$

i.e., $\mathbf{u}_0^i$ satisfies the following normalization condition:

$$\mathbf{u}_0^{i\top} \mathbf{M} \mathbf{u}_0^i = 1 \tag{9}$$

The participation factor Γ^i corresponding to $\mathbf{u}_0^i$ is given as

$$\Gamma^i = \mathbf{u}_0^{i\top} \mathbf{M} \mathbf{I} \tag{10}$$

Assuming that $\mathbf{u}_0^i$ is the vibration mode at the i th step, the generalized displacement and acceleration, denoted by c_{u}^i and c_{a}^i, respectively, at the i th step are obtained by premultiplying $\mathbf{u}_0^{i\top} \mathbf{M}$ to $\mathbf{u}^i$ and $\mathbf{a}^i$ as

$$c_{\mathrm{u}}^i = \mathbf{u}_0^{i\top} \mathbf{M} \mathbf{u}^i, \; c_{\mathrm{a}}^i = \mathbf{u}_0^{i\top} \mathbf{M} \mathbf{a}^i \tag{11}$$

Furthermore, $\mathbf{u}^i$ and $\mathbf{a}^i$ are approximated by $\mathbf{u}_0^i$ in a similar manner as Eq.(4a,b) as

$$\mathbf{u}^i = \Gamma^i D^i \mathbf{u}_0^i, \; \mathbf{a}^i = \Gamma^i A^i \mathbf{u}_0^i \tag{12}$$

with the representative displacement D^i and acceleration A^i. From Eqs.(9), (11), and (12), we obtain

$$D^i = \frac{c_{\mathrm{u}}^i}{\Gamma^i},\ A^i = \frac{c_{\mathrm{a}}^i}{\Gamma^i} \tag{13}$$

Accordingly, the equivalent period T_{eq}^i is defined as

$$T_{\mathrm{eq}}^i = 2\pi\sqrt{\frac{D^i}{A^i}} \tag{14}$$

The proposed approach is similar to the displacement-based adaptive CSM [4], because the actual displacements are used for computing representative responses. However, important point here is that the representative acceleration is defined without using the base shear, because higher modes of an arch do not have large horizontal base shear.

3.2 Estimation of Inelastic Response

The energy dissipation due to plastification is incorporated using the technique of equivalent linearization. Pushover curve between D^i and A^i is approximated by a bilinear relation.

Let D_{y} and A_{y} denote the values of D^i and A^i at the yield point when the first plastification occurs. The equivalent damping coefficient h_{eq} is defined using the plasticity factor $\mu = D^i / D_{\mathrm{y}}$ as

$$h_{\mathrm{eq}} = h + \kappa h_{\mathrm{eq}}^{\mathrm{p}},\ h_{\mathrm{eq}}^{\mathrm{p}} = \frac{2(\mu-1)(1-\gamma)}{\pi\mu(1+\gamma\mu-\gamma)} \tag{15}$$

where h is the initial damping ratio, $h_{\mathrm{eq}}^{\mathrm{p}}$ is the equivalent damping ratio due to plastification, and γ is the ratio of stiffness after yielding to the initial stiffness. The parameter κ is the damping modification factor in ATC-40 [19], which is classified to three types A, B, and C depending on the ductility of the structure.

As demonstrated in the numerical examples in the next section, it is difficult to estimate the mean-maximum dynamic responses under several seismic motions using a single pushover analysis especially for the case with multiple dominant modes. Therefore, we carry out pushover analyses using several load patterns defined by the coefficients $(\alpha_1,\dots,\alpha_N)$ and find the maximum values among those responses.

The inelastic responses are evaluated as follows:

[Step 1:] Define p load patterns by the coefficients $(\alpha_1^{(k)},\dots,\alpha_N^{(k)})$ $(k=1,\dots,p)$. Initialize the load-pattern number as $k=1$.

[Step 2:] Carry out pushover analysis for the k th load pattern.

[Step 2-1:] Initialize the step number as $i=0$.

[Step 2-2:] Increase the load factor for the k th load pattern by the specified value, and let $i \leftarrow i+1$. Update (D^i, A^i) in the representative displacement-acceleration plane.

[Step 2-3:] Go to Step 2-6, if (D^i, A^i) goes beyond $(S^{\mathrm{d}}, S^{\mathrm{a}})$. Go to Step 2-2 if all members are in elastic range; otherwise, define the yield point as $(D_{\mathrm{y}}, A_{\mathrm{y}}) = (D^i, A^i)$.

[Step 2-4:] Increase the load factor, and let $i \leftarrow i+1$. Compute the plasticity factor from the bilinear relation.

[Step 2-5:] Let ω_{eq}^i denote the circular natural frequency corresponding to T_{eq}^i. Compute γ, μ, h_{eq}, and re-calculate the response spectra $S^{\mathrm{d}}(\omega_{\mathrm{eq}}^i)$ and $S^{\mathrm{a}}(\omega_{\mathrm{eq}}^i)$, which depend on the damping coefficient. Go to Step 2-4, if (D^i, A^i) does not go beyond $(S^{\mathrm{d}}, S^{\mathrm{a}})$.

[Step 2-6:] Find the intersection point between the pushover curve and response spectrum, and output the absolute value of each response, which is represented by $R_j^{\mathrm{s}(k)}$ for the j th response quantity, at the intersection point.

[Step 3:] Let $k \leftarrow k+1$ and go to Step 2, if $k \le p$. Otherwise, find the maximum value among the responses to p load patterns $R_j^{\mathrm{s}(k)}$ $(k=1,\dots,p)$ for each response quantity.

This way, the approximate maximum responses can be found if the load patterns are appropriately defined.

The use of elastic eigenmodes for inelastic deformation does not mean that the eigenmodes do not change after yielding. The modes are used only as bases of expanding the deformation and acceleration.

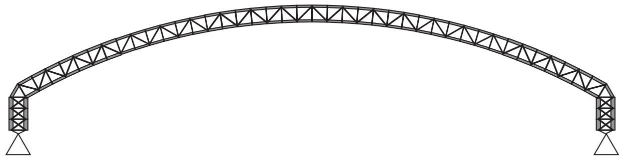

Figure 1. *An arch-type pin-jointed truss model.*

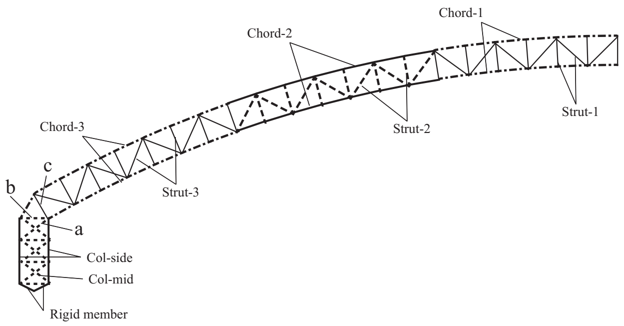

Figure 2. *Member groups.*

Table 1. *Cross-sectional areas of member groups.*

Member group	Cross-sectional area (m^2)	Member group	Cross-sectional area (m^2)
Chord-1	5.341×10^{-3}	Strut-1	1.524×10^{-3}
Chord-2	4.835×10^{-3}	Strut-2	1.083×10^{-3}
Chord-3	6.333×10^{-3}	Strut-3	1.524×10^{-3}
Col-side	9.839×10^{-3}	Col-mid	1.524×10^{-3}

4. NUMERICAL EXAMPLES

4.1 Arch-type truss model

Maximum responses of an arch-type pin-jointed truss as shown in Fig. 1 are found for verification of the proposed method. The model is a slight modification of the arch-type truss in [21]. The lower columns are also modeled as pin-jointed trusses. The span length is $80\ \mathrm{m}$, the open angle of the lower circle of the arch is $2\pi/9$, and the difference between the radii of the lower and upper circles is $2.0\ \mathrm{m}$. The height and width of the column are $4.5\ \mathrm{m}$ and $2.0\ \mathrm{m}$, respectively.

The members of arch and column are classified to nine groups as shown in Fig.2. The cross-sectional areas of member groups are listed in Table 1, except the rigid members connected to the pin support, for which sufficiently large areas are given.

The material of all members is steel, where the elastic modulus is $205.0\ \mathrm{kN/mm^2}$, the yield stress is $235.0\ \mathrm{N/mm^2}$, and the hardening coefficient is 1/100. The nodal masses are $1800.0\ \mathrm{kg}$ for four nodes at the exterior side of each column, and $1600.0\ \mathrm{kg}$ for the lower nodes of arch. Note that the nodal mass is assumed to include the mass of steel members.

The frame analysis program OpenSees Ver. 2.2.2 [22] is used for inelastic static/dynamic analysis. The arch-type truss is subjected to horizontal excitation. The responses due to vertical excitation and self-weight are not considered for simple presentation of the proposed method. The Rayleigh damping is used with the damping ratio 0.02 for the two lowest antisymmetric modes that are excited by horizontal motion.

The design acceleration response spectrum is specified by Notification 1461 of MLIT, Japan, corresponding to the performance level of life safety. The amplification factor G for the ground of second rank and the definition of F defined in Notification 1457 of MLIT is used. Then the design response acceleration spectrum S^{a} $(\mathrm{m/s^2})$ is defined as follows for a ground of second rank:

$$S^{\mathrm{a}} = aFA_0\,,\quad F = \frac{1.5}{1+10h_{\mathrm{eq}}}\,,$$

$$A_0 = \begin{cases} 0.96 + 9T_{\mathrm{eq}} & T < 0.16 \\ 2.4 & 0.16 \le T_{\mathrm{eq}} < 0.864 \\ 2.074/T_{\mathrm{eq}} & 0.864 \le T_{\mathrm{eq}} \end{cases} \tag{16}$$

where T_{eq} (s) is the equivalent natural period, A_0 $(\mathrm{m/s^2})$ is the acceleration response spectrum for $h = 0.05$, and a is the intensity factor, which is equal to 7.5 in the following examples.

The three lowest antisymmetric eigenmodes are illustrated in Fig. 3. Note that the 2nd and 4th modes are symmetric with respect to the center axis and are not excited by a horizontal motion. The values of T_n, Γ_n, ρ_n, S_n^{a}, and E_n of each mode is listed in Table 2. As seen from Table 2, the sum of

ρ_n of the 1st and 3rd modes is 0.8871, which is close to the total sum 1.0, and ρ_n of the 5th mode is very small. However, as shown in the following example, the 5th mode may be indispensable for evaluation of force and stress responses. Therefore, we consider the three lowest antisymmetric modes in the following.

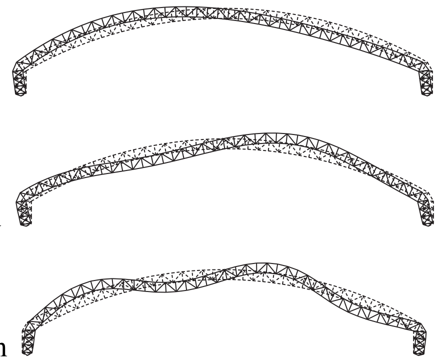

Figure 3. *Three lowest antisymmetric eigenmodes.*

Table 2. *Values of T_n (s), Γ_n, ρ_n, S_n^{a} (m/s^2), and E_n (kNm) of the arch-type truss.*

Mode	T_n	Γ_n	ρ_n	S_n^{a}	E_n
1	1.054	216.8	0.5874	15.37	3999
2	0.6955	0.0	0.0	---	---
3	0.3420	154.8	0.2997	18.75	319.7
4	0.2758	0.0	0.0	---	---
5	0.1800	56.62	0.04007	17.14	9.900

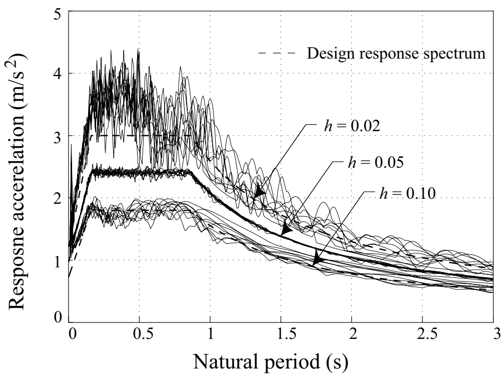

Figure 4. *Design acceleration response spectrum and response spectra of artificial motions for $h = 0.02$, 0.05, and 0.10.*

4.2 Time-History Analysis

In order to investigate accuracy of the pushover analysis, dynamic responses are found for ten artificial ground motions that are compatible to the acceleration response spectrum in Eqs.(16) with $h = 0.05$. The waves are generated using the standard approach of assemblage of sinusoidal waves. The response spectra for various damping ratios are shown in Fig. 4.

The Newmark-β method with $\beta = 1/4$ is used for analysis with the time increment $0.01\,\mathrm{s}$. Fig. 5(a) and (b) show the modal displacement response $\Gamma_n D_n$, defined in Eq.(4), for modes 1 and 3 for two of the ten artificial waves. The response for mode 5 is omitted, because it is very small. As is seen, the lowest mode dominates in displacement response even in the inelastic range.

Fig. 6 shows the modal acceleration response $\Gamma_n A_n$, defined in Eq.(4), for modes 1, 3, and 5 for two of the ten artificial waves. As is seen, the higher modes including mode 5 dominate in the acceleration response. Similar properties can be observed for wave 2.

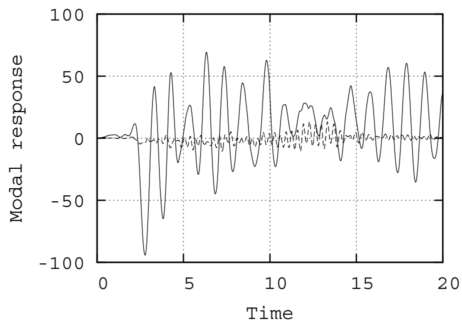

(a)

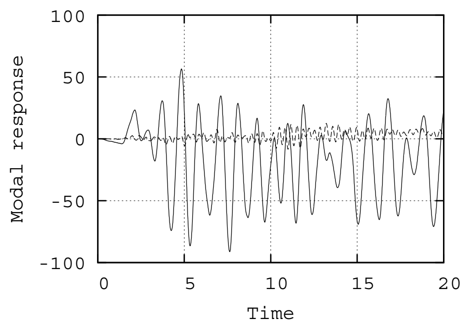

(b)

Figure 5. *Time histories of modal displacement responses; solid line: mode 1, dotted line: mode 3; (a) wave 1, (b) wave 2.*

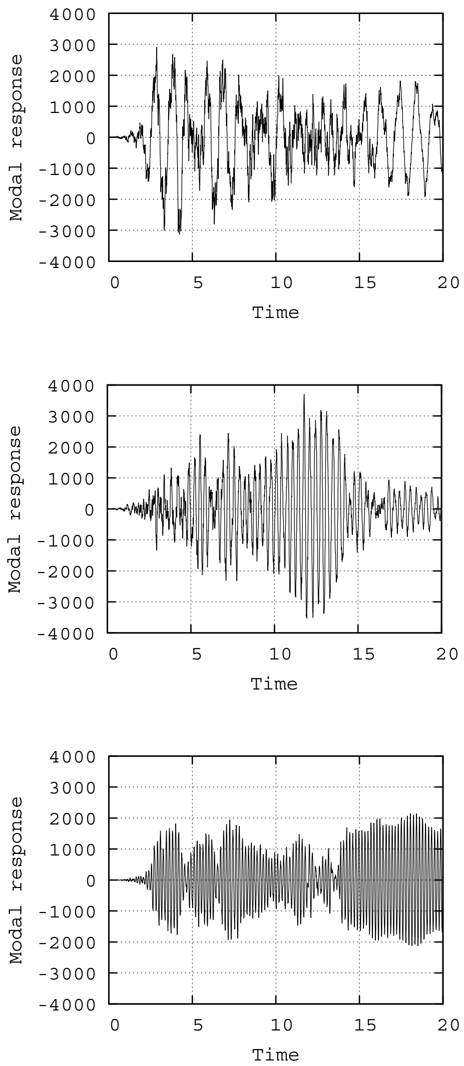

(a)

(b)

(c)

Figure 6. *Time histories of modal acceleration responses for wave 1; (a) mode 1, (b) mode 3, (c) mode 5.*

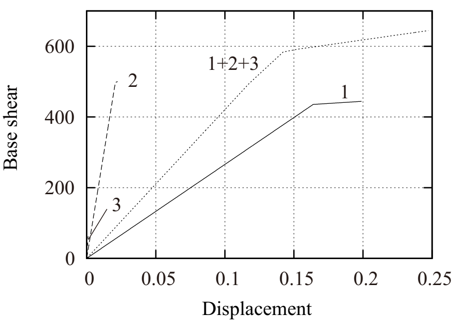

Figure 7. *Relation between horizontal displacement of center and base shear.*

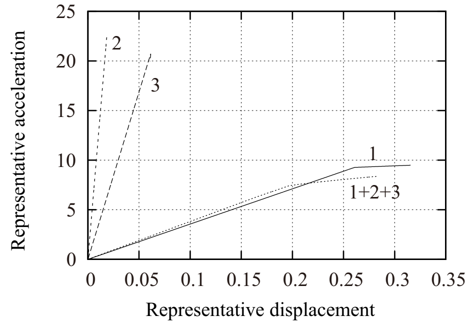

Figure 8. *Relation between generalized displacement and acceleration.*

4.3 Pushover analysis

We first carry out pushover analysis using the load pattern proportional to each of modes 1, 3, and 5, and investigate the applicability of bilinear approximation of the pushover curve. The initial damping ratio is 0.02, and the Type-A in ATC-40 [21] with stable hysteresis is used for definition of damping modification factor κ , because member buckling is ignored and the stress-strain relation is assumed to have a full loop.

Fig. 7 shows the relation between the horizontal displacement of the center node and the base shear for modes 1, 3, 5, and their summation $(\alpha_1,\alpha_3,\alpha_5)=(1,1,1)$. Fig. 8 shows the relation between the representative displacement and acceleration for the same load patterns as Fig. 7. As is seen from these figures, each curve may be approximated by a bilinear relation with good accuracy. However, the rates of plasticity are different depending on the load pattern; therefore, it will be difficult to combine inelastic responses of each mode, as demonstrated in the numerical examples, to obtain the total responses. Note that the yield point is numerically detected in the following pushover analysis as the point where the tangent stiffness in the (D^i, A^i) space is less than half of its initial value.

Furthermore, the contributions of higher modes in Fig. 8 are larger than those in Fig. 7, because the higher modes have mainly vertical displacements and do not contribute to the base shear, and they do not yield simultaneously.

It is not straightforward to define the initial damping ratio h in Eq.(15) for a multimodal pushover analysis, because the generalized displacement and acceleration are combinations of multiple modes that have different damping ratios. In the example below, the smallest value 0.02 is used in the process of equivalent linearization.

Let R_i^{d} denote the mean value of the maximum absolute value of the i th response quantity under ten seismic motions. We carry out pushover analyses with p different load patterns to obtain the absolute values of static responses $R_i^{\mathrm{s}(k)}$ $(k = 1,\ldots,p)$. Then, approximation ratio C_i is defined as follows for the i th response quantity:

$$C_i = \max_k \frac{R_i^{\mathrm{s}(k)}}{R_i^{\mathrm{d}}} \tag{17}$$

The pushover analysis overestimates (underestimates) the response if $C_i > 1$ ($C_i < 1$), and good approximation is achieved if $C_i \simeq 1$. Since approximation ratios of horizontal displacements (H-disp.), vertical displacements (V-disp), and stresses are different depending on displacement components and members over the total structure, the mean, maximum, minimum, and standard deviation are computed for those responses, respectively.

We first discretize the coefficients α_1 , α_3 , and α_5 into five values $(-1.0, -0.5, 0.0, 0.5, 1.0)$. Therefore, we have $5^3 = 125$ load patterns. The results for all load patterns are listed in the first part, indicated by ‘All’, in Table 3. Note that the four vertical displacements that are less than 0.01 m are excluded, and only 116 stresses that are greater than a half of the yield stress is evaluated.

As is seen, the pushover analysis overestimates some displacement and stress components, and the standard deviation is rather large, although a good accuracy is achieved for the base shear. Furthermore, it is not practically acceptable to carry out analysis 125 times. Therefore, we reduce the number of sampling values to three as $(-1.0, 0.0, 1.0)$; i.e., the total number is reduced to $3^3 = 27$.

Table 3. *Results of pushover analysis of inelastic structure.*

		H-disp.	V-disp.	Stress	Base shear
All	Mean	0.9687	0.8827	1.093	1.0277
	Std. dev	0.1530	0.1901	0.0978	
	Max.	1.344	1.295	1.346	
	Min.	0.8342	0.6998	0.8473	
Case 13	Mean	0.8977	0.8211	0.9367	0.9961
	Std. dev	0.1037	0.1169	0.0934	
	Max.	1.172	1.068	1.077	
	Min.	0.7894	0.6899	0.7030	
Case 9	Mean	0.8977	0.8210	0.9084	0.9961
	Std. dev	0.1037	0.1169	0.1433	
	Max.	1.172	1.068	1.077	
	Min.	0.7894	0.6899	0.4438	
Mode 1	Mean	0.7043	0.7142	0.6951	0.6865
	Std. dev	0.0097	0.0181	0.2386	
	Max.	0.7199	0.7430	0.9697	
	Min.	0.6609	0.6843	0.0135	
Mode 3	Mean	0.0879	0.1319	0.4340	0.7733
	Std. dev	0.0482	0.0773	0.2435	
	Max.	0.1892	0.2395	0.9529	
	Min.	0.0396	0.0005	0.0098	
Mode 5	Mean	0.0049	0.0199	0.0928	0.1117
	Std. dev	0.0035	0.0100	0.0647	
	Max.	0.0186	0.0367	0.2400	
	Min.	0.0000	0.0001	0.0011	
MPA	Mean	0.7114	0.7210	0.8872	1.040
	Std. dev	0.0102	0.0688	0.1159	
	Max.	0.7261	0,7670	1.260	
	Min.	0.6822	0.2818	0.6591	

It should also be noted that there are many identical load patterns in the set of 27 patterns; e.g., $(\alpha_1, \alpha_3, \alpha_5) = (1, 0, -1)$ and $(-1, 0, 1)$ lead to the same result for the symmetric arch-type truss. Therefore, the load patterns can be reduced to 13 to obtain the results in the second part (Case 13) of

Table 3. In this case, all the responses are slightly smaller than those for the case 'All' with five sampling values.

In order to further reduce the number of analyses, we assume that the 1st mode should always be included. Hence, the load patterns are reduced to nine as (1, 1, 1), (1, 1, 0), $(1,1,-1)$, (1, 0, 1), (1, 0, 0), $(1,0,-1)$, $(1,-1,1)$, $(1,-1,0)$, $(1,-1,-1)$. The results are listed in the third part (Case 9) of Table 3, which are almost the same as Case 13. This indicates that the 1st mode should be included in the load pattern at the maximum deformation even for the evaluation of maximum stresses and base shear. The single-mode responses are also listed as 'Mode 1, 3, 5' in Table 3, which obviously do not have good accuracy. The MPA [7] is carried out for comparison purpose, where the modal responses obtained by the load patterns (1,0,0), (0,1,0), and (0,0,1) are combined by the SRSS rule. As shown in the last part of Table 3, the MPA underestimate displacements.

Table 4. *Comparison of estimated stresses* ($\mathrm{N/mm^2}$) *and its ratio to dynamic response of yielded members.*

	All		Case 13		Case 9	
	stress	ratio	Stress	ratio	Stress	ratio
a	256.4	1.054	255.4	1.050	255.4	1.050
b	270.3	1.083	269.4	1.077	269.4	1.077
c	298.1	1.202	256.1	1.033	256.1	1.033
	Mode 1		Mode 3		Mode 5	
	Stress	Ratio	Stress	Ratio	Stress	Ratio
a	146.1	0.6007	153.6	0.6314	19.41	0.07980
b	227.4	0.9089	220.8	0.8826	24.40	0.09750
c	146.9	0.5922	240.3	0.9691	47.79	0.1928
	MPA		MPA2			
	Stress	Ratio	Stress	Ratio		
a	211.0	0.8676	211.0	0.8676		
b	315.3	1.260	235.8	0.9425		
c	282.3	1.139	235.5	0.9497		

In order to investigate more details of the stress responses, the stresses of the yielded members 'a', 'b', and 'c', which are indicated in Fig. 2, are listed in Table 4. Note that the yielding is detected by the mean values of the dynamic responses. As is seen, mode 1 dominates in the stress responses of member 'b', while modes 3 dominates for members 'b' and 'c'. Member 'c' yields for mode 3, and the remaining single-mode responses are all in elastic range. Furthermore, mode 5 cannot be neglected, because it has some effect on member 'c', although it does not dominate in any of these three members. Consequently, the MPA overestimates the stresses, because it cannot incorporate the reduction of stiffness due to yielding in the process of SRSS combination. In contrast, Cases 13 and 9 can estimate the stresses with good accuracy, because yielding is appropriately taken into account in the process of pushover analysis utilizing the load pattern with combined modes.

The maximum value 1.260 for MPA in Table 3 indicates that the stress of a yielded member is overestimated, while the minimum value 0.7030 for Case 9 corresponds to underestimate of the stress of a member with small value. It should be noted that accuracy of stresses of yielded members is more important than that with small values. If we use the extended MPA, which estimates stresses by local correction utilizing the stress-strain relation [9], we considerably underestimate the stresses as shown in the last column of MPA2 in Table 4.

5. CONCLUSIONS

A static analysis procedure has been presented for evaluation of the mean-maximum inelastic seismic responses of long-span structures subjected to seismic motions. Representative displacement and acceleration are defined assuming that the displacement response at each step of pushover analysis represents a vibration mode. This way, the representative responses can be defined in a general manner for long-span structures for which the base shear and roof displacement that are used for regular building frames are not applicable.

Pushover analyses are carried out several times for the specified set of load patterns, and inelastic responses are found using equivalent linearization. Since more than one mode dominate in the seismic responses of long-span structures, each load pattern is defined as a combination of multiple modes. However, the number of analyses will very large if many modes dominate; therefore, we restrict application of our approach to the case where at most three modes dominates.

Numerical studies on an arch-type truss model have shown that the proposed method has good performance in estimating the mean-maximum inelastic responses including stresses and base shear. However, further investigation is needed to find appropriate set of modal combinations to reduce the number of load patterns. The methods of design of experiments can be effectively used for this purpose.

REFERENCES

[1] **Kato, S., Nakazawa, S., and Saito, K.,** Estimation of static seismic loads for latticed domes supported by substructure frames with braces deteriorated due to buckling, J. IASS., Vol. 48(2), pp. 71-86, 2007.

[2] **Takeuchi, T., Ogawa, T., and Kumagai, T.,** Seismic response evaluation of latice shell roofs using amplification factors, J. Int. Assoc. Shell and Spatial Struct., Vol. 48(3), pp. 197-210, 2007.

[3] **Wilson, E.L., Der Kiureghian, A., and Bayo, E.P.,** A replacement of the SRSS method in seismic analysis. *Earthquake Eng. Struct. Dyn.*, Vol. 13, pp. 1-12, 1982.

[4] **Casarotti, C., and Pinho, R.,** An adaptive capacity spectrum method for assessment of bridges subjected to earthquake action, *Bulletin of Earthquake Eng.*, Vol. 5(3), pp. 377-390, 2007.

[5] **Bracci, J.M., Kunnath, S.K., and Reinhorn, A.M.,** Seismic performance and retrofit evaluation for reinforced concrete structures, *J. Struct. Engng.*, Vol. 123(1), pp. 3-10, 1997.

[6] **Gupta, G., and Kunnath, S.K.,** Adaptive spectra-based pushover procedure for seismic evaluation of structures, *Earthquake Spectra*, Vol. 16(2), pp.367-392, 2000.

[7] **Chopra, A.K., and Goel, R.K.,** A modal pushover analysis procedure for estimating seismic demands for buildings, *Earthquake Eng. Struct. Dyn.*, Vol. 31, pp. 561-582, 2002.

[8] **Reyes, J.C., and Chopra, A.K.,** Three-dimensional modal pushover analysis of buildings subjected to two components of gqound motion, including its evaluation for tall buildings, *Earthquake Eng. Struct. Dyn.*, Vol. 40, pp. 789-806, 2011.

[9] **Goel, R.K. and Chopra, A.K.,** Extension of modal pushover analysis to compute member forces, *Earthquake Spectra*, Vol. 21(1), pp. 125-139, 2005.

[10] **Kunnath, S.K.,** Identification of modal combinations for nonlinear static analysis of building structures, *Computer-Aided Civil and Infrastructure Eng.*, Vol. 19, pp. 246-259, 2004.

[11] **Park, H.G., Eom, T., and Lee, H.,** Factored modal combination for evaluation of earthquake load profiles, *J. Struct. Engng.*, Vol. 133(7), pp. 956-968, 2007.

[12] **FEMA-356,** *NEHRP Guidelines for the Seismic Rehabilitation of Buildings*, Building Seismic Safety Council, Washington DC, 2000.

[13] **European Committee for Standardization (CEN),** *Eurocode 8: Design of structures for earthquake resistance, Part 1: General rules, seismic actions and rules for buildings (EN 1998-1: 2004)*, Brussel, 2004.

[14] **Chopra, A.K., and Goel, R.K.,** Capacity-demand-diagram methods for estimating seismic deformation of inelastic structures: SDF systems, *Technical Report Report No. PEER-1999/02. PEERC*, Univ. California, Berkeley, 1999.

[15] **Freeman, S.A.,** Review of the development of the capacity spectrum method. *ISEL Journal of Earthquake Technology*, Vol. 41(1), pp. 1-13, 2004.

[16] **Nakazawa, S., Kato, S., Yoshino, T, and Oda, K.,** Study on seismic response estimation based on pushover analysis for membrane structure supported by substructure, *Proc. Int. Symposium of IASS*, Bucharest and Poiana Brasov, Romania, 2005.

[17] **Kato, S., Nakazawa, S., and Saito, K.,** Two-modes pushover analysis for reticular domes for use of performance based design for estimating responses to severe earthquakes, *Proc. Int. Symposium of IASS*, Bucharest and Poiana Brasov, Romania, 2005.

[18] **Uchida, A., Ohsaki, M., and Zhang, J.Y.,** Prediction of inelastic seismic responses of spatial structures by static analysis with higher modes, *J. Struct. Eng., AIJ*, Vol. 55B, pp. 49-56, 2009. (in Japanese).

[19] **Zhang, J.Y., Ohsaki, M., and Uchida, A.,** Equivalent static loads for nonlinear seismic design of spatial structures, *Proc. 14th World Conf. on Earthquake Eng.*, Paper No. 05-01-0110, Beijing, 2008.

[20] **ATC-40, Applied Technology Council,** *Seismic evaluation and retrofit of concrete buildings*, Report ATC 40, 1996.

[21] **Kato, S., Nakazawa, S., and Gao, X.,** Elastic seismic responses and equivalent static seismic forces of large span arches, *J. Struct. Eng., AIJ*, Vol. 55B, pp. 49-56, 2002. (in Japanese).

[22] **PEERC,** *Open System for Earthquake Engineering Simulation (OpenSees),* UCB, CA, 2006. (available at http://opensees.berkeley.edu/).